

# Performance of Underwater Quantum Key Distribution with polarization encoding

SHI-CHENG ZHAO, XIN-HONG HAN, YA XIAO, YUAN SHEN, YONG-JIAN GU\* AND WEN-DONG LI\*

*Department of Physics, Ocean University of China, Qingdao 266100, China.*

E-mail: : yjgu@ouc.edu.cn, liwd@ouc.edu.cn

Underwater quantum key distribution (QKD) has potential applications for absolutely secure underwater communication. However, the performance of underwater QKD is limited by the optical elements, the background light and dark counts of the detector. In this paper, we propose a modified formula of the quantum bit error rate (QBER), in which the effect of detector efficiency on QBER caused by the background light is considered. Then we calculate the QBER of the polarization coding BB84 protocol in Jerlov type seawater by analyzing the effect of background light and optical components in closer to reality situation. Lastly we further analyze the final key rate and the maximum secure communication distance in three propagation modes i.e., upward, downward and horizontal modes. We find that secure QKD can be carried out in the clearest Jerlov type seawater at a distance of hundreds of meters, even in the worst downward propagation mode. Specifically, by optimizing the system parameters, it is possible to securely transmit information with a rate of 67kbits/s at the distance of 100 meters in the seawater channel with a attenuation coefficient 0.03/m at night, and the maximum secure distance can attain more than 300m. For practical underwater QKD, the performance can be improved if decoy state is used according to the calculated secure bit rate for underwater QKD. Our results are helpful to long distance underwater quantum communication.

## 1. Introduction

Underwater communication is vital for underwater sensor networks, submarines, and all kinds of underwater vehicles and the security of which can be provided by quantum key distribution (QKD). QKD enables two remote parties to set up secure keys, whose security is based on the basic physical properties of quantum states, rather than relying on the computational intractability of certain mathematical functions in traditional cryptography. In 1984, Bennett and Brassard proposed the first QKD protocol [1], whose absolute security has been proved using the one-time pad encryption [2–4]. Since the first QKD experiment in 1989 [5] with a distance of 32 cm, a strong research effort has been devoted to achieve practical QKD. At present, great progress has been made in QKD in free space and optical fiber [6–8]. In 2016, a low-earth-orbit satellite to implement decoy state QKD was launched [9], successfully realizing satellite-to-ground QKD over a distance of 1200km with over kHz key rate [10, 11].

However, little breakthrough has been made in underwater QKD in spite of the following

works. The underwater QKD was first proposed in 2010, and the feasibility of underwater quantum communication was briefly proved [12, 13]. In 2014, Monte Carlo simulation was used to study the propagation characteristics of polarized photons in seawater [14], and the effect of underwater channel on QKD was analyzed. These studies showed that secure QKD can be achieved with a distance of one hundred meters in the clearest seawater. L J et al. completed the first experiment of underwater quantum communications in Jerlov type seawater channel [15], which showed polarization qubit and entanglement can maintain well after going through seawater channel and therefore experimentally confirmed the feasibility of underwater quantum communication. The influence of imperfect optical elements on the polarization states for polarization encoding underwater QKD has never been analyzed and the influence of background light on the QBER is not clearly.

In this paper, the quantum bit error rate(QBER) and the final key rate are calculated by analyzing the effect of background light and optical components with a modified QBER formula in three propagation modes(i.e. upward, downward and horizontal). We firstly modified the formula calculating the QBER for a QKD system because the previous formula of the QBER ignores the influence of detection efficiency and optical element transmittance on background light. Then we calculate the background light of the underwater channel with Hydrolight [16] and analyze the effect of the optical elements, whose effect on underwater QKD has never been investigated, in a typical underwater BB84 system with polarization coding. We investigate the QBER to evaluate the performance of underwater QKD and the main factors that affect the QBER of underwater QKD according to the modified formula. At last, we calculate the sifted key rate and final key rate for underwater QKD in the clearest Jerlov type seawater. The results show that the final key rate can reach tens of kbps for the downward and horizontal modes at a distance of 100m and the maximum secure distance can reach hundreds of meters. The performance can be improved if decoy state is used according to the calculated secure bit rate for underwater QKD.

## 2. QBER OF BB84 PROTOCOL

QBER, the ratio of wrong bits to the total bits, is an important parameter in a quantum key distribution system. For a typical free-space polarization coding BB84 system,bit errors are induced by the imperfection of optical elements, the dark count of the single-photon detectors and the background light. According to Ref. [17, 18], the QBER reads

$$QBER = \frac{P \frac{\mu\eta}{2\Delta t} e^{-\chi_c r} + I_{dc} + \frac{LA\Delta t' \lambda \Delta \lambda \Omega}{4hc\Delta t}}{\frac{\mu\eta}{\%2\Delta t} e^{-\chi_c r} + 2I_{dc} + \frac{LA\Delta t' \lambda \Delta \lambda \Omega}{2hc\Delta t}}, \quad (1)$$

where  $P$  is the polarization contrast of the orthogonal states,  $\mu$  is the mean photon number per pulse,  $\eta$  is the detector efficiency,  $\Delta t$  is the bit period,  $\chi_c$  is the attenuation coefficient,  $r$  is the transmission distance,  $I_{dc}$  is the dark counts per second for the detector,  $L$  is the spectral radiance of environment,  $A$  is the receiver aperture,  $\Delta t'$  is the gate time,  $h$  is the Planck constant,  $c$  is the speed of light in vacuum,  $\Delta\lambda$  is the filter spectral width, and  $\Omega = 2\pi(1 - \cos(\gamma/2))$ , which is the solid angle of the field of view(FOV),  $\gamma$  is the FOV of the receiver.

In Eq. 1,  $\frac{LA\Delta t' \lambda \Delta \lambda \Omega}{4hc\Delta t}$  is the detected photon number of background light for each detector, which ignores the effect of the detector efficiency. The efficiency include the quantum efficiency  $\eta$  of the detector and the transmittance  $\eta_{opt}$  of optical elements in the receiver. So the detected background light will be  $\frac{LA\Delta t' \lambda \Delta \lambda \Omega \eta \eta_{opt}}{4hc\Delta t}$ . Besides, scattering in the ocean and its effects on the polarization of scattered photons should also be considered. Then the sources of wrong bits will include: depolarized photons caused by optical elements, depolarized photons due to scattering, dark counts and detected background light. So, the QBER formula (Eq. 1) should be modified to

$$QBER = \frac{P \frac{\mu\eta\eta_{opt}}{2\Delta t} e^{-\chi_c r} + P_s N + I_{dc} + \frac{LA\Delta t' \lambda \Delta \lambda \Omega \eta \eta_{opt}}{4hc\Delta t}}{\frac{\mu\eta\eta_{opt}}{2\Delta t} e^{-\chi_c r} + N + 2I_{dc} + \frac{LA\Delta t' \lambda \Delta \lambda \Omega \eta \eta_{opt}}{2hc\Delta t}}, \quad (2)$$

where  $N$  is the number of the scattered photons received by the detector,  $P_s$  is the probability of the scattered photons that cause errors, and  $\eta_{opt}$  is the transmission of optical elements. The influence of the scattered photons has been studied in [14] through Monte Carlo method, and the results indicate that the majority of the scattered photons could be well filtered by small FOV and aperture, so the change of the QBER caused by the scattering of photons is extremely small, thereby negligible. In the following sections, we will detailed analyze the QBER caused by the background light in different types of water, the optical elements on polarization, respectively.

### 3. ANALYSIS OF BACKGROUND LIGHT

The underwater background light is mainly come from the direct incidence and reflection of the sunlight, which varies with the time, the location, the turbidity of seawater, the detection direction, etc. The intensity of the background light is qualified by spectral radiance, which indicates the energy emitted from the unit area of a surface radiation source in the unit solid angle and unit time [16, 19].

The long distance effective key distribution is restricted because of severe attenuation in turbid seawater. However, there is a blue-green optical window of seawater [16]. So we calculate the spectral radiance with the wavelength of 480nm in three different radiation directions (upward, downward and horizontal) at night for several lunar phase angles in Jerlov type seawater which is a type of clear open ocean water. The upward mode means the propagation direction of the quantum signal is upward, the receiver is downward and immovable (in our case, 1m below the sea level), and the signal transmitter moves down to change the propagation distance. The downward mode means the propagation direction of the signal is downward. The transmitter remains stationary and the receiver moves downward. The horizontal mode means the signal transmitter and receiver are located at 100m under the sea level and the signal is propagated along the horizontal direction. When calculating the background light with Hydrolight, the phase function we select is 'average particle' and the bottom model is 'average seagrass'. The results are illustrated in Fig. 1.

Fig. 1(a), (b) and (c) show the spectral radiance of background light is as a function of depth in Jerlov type-I seawater, with the attenuation coefficient of 0.03/m, for different lunar phase angles (full moon, Gibbous and quarter). The results of Jerlov type-II seawater, with the attenuation coefficient of 0.18/m, are presented in Fig. 1 (d), (e) and (f).

It is obvious that the spectral radiation decreases with the increase of depth and the spectral radiance under full moon condition is the maximum. The spectral radiance magnitude of downward background light is maximal among the three modes which is about one or two orders higher than that of the other two modes. The downward light is the downward component of the environmental light incident into the water, and the horizontal and upward light are generated from environmental light due to the scattering of particulate matters in water and the reflection of the sea floor. For clear ocean water, the scattered light is at a low level comparing to the total light. In general, the spectral radiance is at a level of  $10^{-9} - 10^{-7} W/(m^2 \cdot sr \cdot nm)$  for most situation and it decreases to a level of about  $10^{-11} W/(m^2 \cdot sr \cdot nm)$  or smaller.

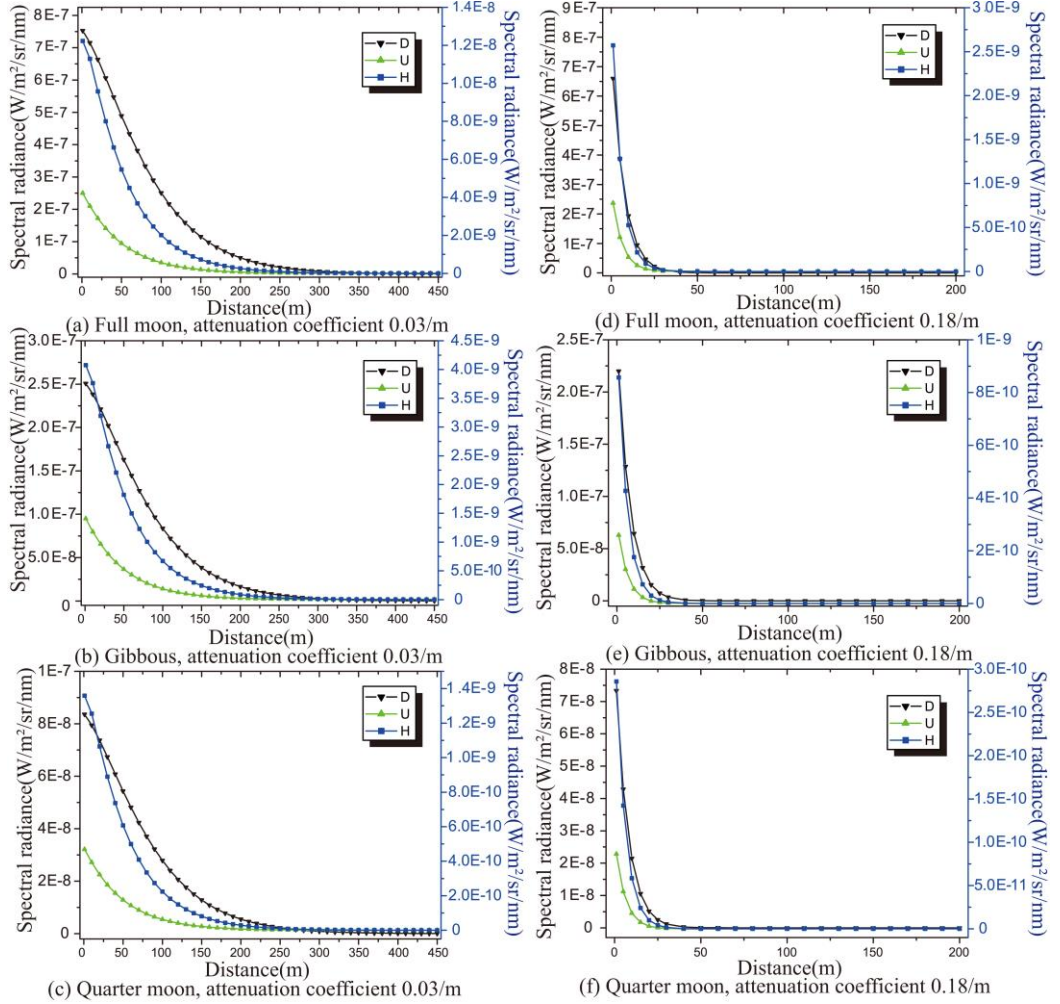


**Fig. 1.** (color online) Spectral radiance curve of underwater background radiance in Jerlov type seawater with respect to different lunar phase angles. The black down triangle (see the left axis), green up triangle, blue box (see the right axis) stand for downward(D), downward(D) and horizontal(H) spectral radiance, respectively.

#### 4. EFFECT OF OPTICAL COMPONENTS

For the polarization coding BB84 protocol, four polarization states will usually be combined by a beam splitter at the transmitter's site and split at the receiver's site. In this paper, the four states we consider are Horizontal(H), Vertical(V),  $45^\circ$  (D) and  $135^\circ$  (M). Considering the four types of polarizations produced by imperfect polarizer and wave plate, in this section, we analyze the influence of beam splitter, imperfect polarizer and wave plate on polarization, and calculate the QBER.

The relationship between the stokes parameters of the incident light beam  $I_0$  and the emerging light beam  $I_1$  after passing through an optical component can be described by a  $4 \times 4$  Mueller matrix [20].

For a BB84 protocol shown in Fig. 2, the H, V states will transmit through the beam splitter and the D, M states are reflected, both at the transmitter and receiver. Then the H, V polarized states reaching the detector follows  $I_1 = M_{p2}M_tM_rM_{p1}I_0$  where  $M_{p1}$  and  $M_{p2}$  represent the Mueller matrix of the polarizer of the transmitter and receiver with an extinction ratio, respectively. The  $4 \times 4$  Mueller matrix of a polarizer with a extinction ratio of  $\varepsilon^2$  is

$$\begin{aligned} M_{11} &= 1 + \varepsilon^2 \\ M_{22} &= (1 + \varepsilon^2) \cos^2 2\theta + 2\varepsilon \sin^2 2\theta \\ M_{33} &= (1 + \varepsilon^2) \sin^2 2\theta + 2\varepsilon \cos^2 2\theta \\ M_{44} &= 2\varepsilon \\ M_{12} &= M_{21} = (1 - \varepsilon^2) \cos 2\theta \\ M_{13} &= M_{31} = (1 - \varepsilon^2) \sin 2\theta \end{aligned} \quad , \quad (3)$$

whose other elements are 0. The D, M polarization states reaching the detector follows  $I_2 = M_{p2}M_{hp2}M_rM_{hp1}M_{p1}I_0$ , where  $M_{hp1}$  and  $M_{hp2}$  represent the Mueller matrix of a half wave plate of the transmitter and receiver with a retardation accuracy,  $M_t$  ( $M_r$ ) represents the Mueller matrix of the beam splitter for the transmitted (reflected) light with transmissivity(reflectivity) of  $tp$  ( $rp$ ) and  $ts$  ( $rs$ ) for the p and s polarization states, and  $\phi t$  ( $\phi r$ ) represents the phase difference of the p and s states for transmitted (reflected) light.

The Mueller matrix of a BS for the transmitted light  $M_t$  is

$$\begin{pmatrix} \frac{1}{2}(t_p + t_s) & \frac{1}{2}(t_p - t_s) & 0 & 0 \\ \frac{1}{2}(t_p - t_s) & \frac{1}{2}(t_p + t_s) & 0 & 0 \\ 0 & 0 & \sqrt{t_p \cdot t_s} \cos \phi_t & -\sqrt{t_p \cdot t_s} \sin \phi_t \\ 0 & 0 & \sqrt{t_p \cdot t_s} \sin \phi_t & \sqrt{t_p \cdot t_s} \cos \phi_t \end{pmatrix}, \quad (4)$$

and the Mueller matrix of a BS for the reflected light  $M_r$  is

$$\begin{pmatrix} \frac{1}{2}(r_p + r_s) & \frac{1}{2}(r_p - r_s) & 0 & 0 & \% \\ \frac{1}{2}(r_p - r_s) & \frac{1}{2}(r_p + r_s) & 0 & 0 & \% \\ 0 & 0 & \sqrt{r_p \cdot r_s} \cos \phi_r & -\sqrt{r_p \cdot r_s} \sin \phi_r & \\ 0 & 0 & \sqrt{r_p \cdot r_s} \sin \phi_r & \sqrt{r_p \cdot r_s} \cos \phi_r & \end{pmatrix}. \quad (5)$$

The Mueller matrix of a wave plate is

$$\begin{aligned} M_{11} &= 1, M_{22} = \cos^2 2\theta + \cos \delta \sin^2 2\theta \\ M_{33} &= \cos^2 2\theta \cos(\delta) + \sin^2 2\theta, M_{44} = \cos \delta \\ M_{23} &= M_{32} = \cos 2\theta \sin 2\theta - \cos 2\theta \cos \delta \sin 2\theta. \\ M_{24} &= -M_{42} = -\sin 2\theta \sin \delta \\ M_{34} &= -M_{43} = \cos 2\theta \sin \delta \end{aligned} \quad (6)$$

where  $\delta$  is the phase difference between the fast and slow axis, and  $\theta$  is the angle of the fast axis, other elements are 0. Typically, for a half wave plate,  $\delta = \pi$ . In practical applications, the extinction ratio of a polarizer can reach 1:10000 [21], and the retardation accuracy of a wave plate can be limited within  $\lambda/300$  [22, 23]. The rotation accuracy of the polarizer and the wave plate is 5 arc minutes, which is easy to realize for the optical mounts(such as PRM1 of Thorlabs). Generally, the H, V polarization states are minimally influenced by a BS. Because the influence of a BS on the polarization states is due to the different transmission(reflection) and the phase difference of the p and s states. In the ordinary case, the  $r_p$  and  $r_s$  are both  $50 \pm 5\%$  and the  $\phi_r$  s about  $7^\circ - 9^\circ$ , then  $P \approx 0.017$ . For the optimized non-polarizing beam splitters, the  $r_p$  and  $r_s$  can reach  $50 \pm 0.5\%$ , and  $\phi_r = (0 \pm 0.3)^\circ$  [24], resulting to  $P \approx 2.3 \times 10^{-4}$ . Also, we will analyze the QBER and key rate under these two situations, an ordinary case and an optimal case, in the following section

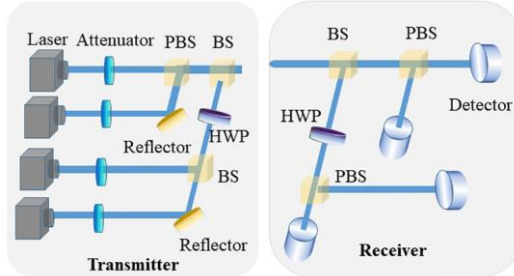


**Fig. 2.** . (color online) Sketch of the transmitter and receiver of a BB84 protocol, the polarized photons will output from the transmitter, propagate through the channel and input into the receiver. HWP represents the half wave plate, PBS represents the polarization Beam Splitter.

## 5. PERFORMANCE ANALYSIS OF UNDERWATER QKD SYSTEMS

QBER is an important indicator of QKD. In this section, we first analyze the main factors affecting the QBER of underwater QKD system. Then, the QBER for different distances is studied for different transmission modes, i.e., upward, downward and horizontal. Finally, the key rates in the three modes are calculated, including the sifted key rate and the final key rate.

### A. Analysis of the QBER of underwater QKD

According to Eq. 2, there are three main factors, i.e., the dark counts, the background light and the misalignment of optical components, contributing to the QBER. The dark counts ( $I_{dc}$ ) and the detection efficiency ( $\eta$ ) of single photon detectors directly determine the quantum key generation rate and distribution distance.  $I_{dc}$ ,  $\eta$  are 100, 20% for an ordinary single photon detector and 1, 80% for the superconducting nanowire single-photon detector. The background light is determined by the environment, as illustrated in Fig. 1. The system parameters used for calculating the QBER and key rate of the ordinary case and the preferable case are listed in Table 1 and Table 2, respectively

**Table 1. System parameters for the ordinary case**

$P = 0.017$	$\Delta\lambda=1nm$	$\eta = 20\%$
$\Delta t' = 5ns$	$I_{dc} = 100$	$f = 40MHz$
$\gamma = 10mrad$	$\mu = 0.1$	$\chi_c = 0.03, 0.18/m$
$\eta_{opt} = 95\%$	$A = 30cm^2$	

**Table 2. System parameters for the optimal case**

$P = 2.3 \times 10^{-4}$	$\Delta\lambda=0.12nm$	$\eta = 80\%$
$\Delta t' = 200ps$	$I_{dc} = 1$	

The same parameters are not listed in Table 2.  $P$  is calculated in section 4,  $\chi_c$  is the attenuation coefficient of the Jerlov type water,  $\Delta\lambda$  in Table 1 is the bandwidth of an ordinary filter(such as the filter made in Thorlabs) and  $\Delta\lambda$  in Table 2 is from Ref. [13],  $f$  is the frequency of the quantum signal [25],  $\eta_{opt}$  is evaluated according to the transmissivity of the optical elements of the receiver in Fig.6,  $A$  is from Ref. [13].

We first analyze the QBER caused by the background light. For a given condition, the

background light received by the detector mainly depends on the propagation direction, the receiver aperture and the FOV. The influences of receiver aperture and FOV under full moon condition in the Jerlov type-I seawater are shown in Fig. 3 (a) and (b), respectively. It is obvious that the QBER increases as the FOV and the receiver aperture increase. It can be seen from Fig. 1 (a) that the intensity of background light is the maximum for downward propagation mode . The secure QKD can be achieved when FOV is less than 11mrad. For the upward and horizontal modes, the QBER increases slowly when the FOV is in the range of 0 to more than 10mrad. When FOV reaches dozens of mrad, the QBER gradually becomes more sensitive to the increase of FOV . The background light becomes the main factor for the QBER. From Fig.3 (b), we can find that the correlation between the QBER and receiver aperture is approximately linear , which is especially obvious for upward and horizontal modes. So we can reduce the QBER induced by the background noise by choosing a smaller FOV effectively, and a small aperture is also helpful to reduce the QBER.

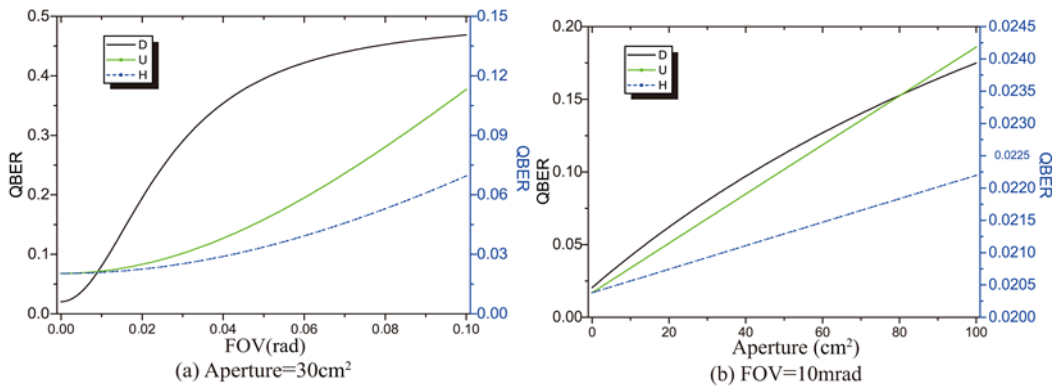


Fig. 3. (color online) (a). QBER as a function of FOV (with a fixed aperture of  $30\text{cm}^2$  ). (b). QBER as a function of aperture (with a fixed FOV of 10 mrad). The black line (left axis) describes the downward mode and the blue and green lines (right axis) describe the other two modes. The transmission distance of the signal is 100 meters. Other system parameters are shown in Table 1.

In order to decrease the influence of background light on underwater QKD, small FOV (10mrad) and Aperture ( $30\text{cm}^2$ ) in the range of secure QKD are selected to investigate the relationship between the QBER and the propagation distance. Fig 4 shows the QBER under the Jerlov type-I seawater caused by the optical elements( $Q_{\text{opt}}$ ), the background light( $Q_{\text{bac}}$ ) and the dark counts( $Q_{\text{Idc}}$ ) under full moon condition. The QBERs in the ordinary case are shown in Fig.4 (a), (b), (c). For long distance underwater QKD, the main source of the QBER is dark counts. It is worth noting that  $Q_{\text{bac}}$  in Fig.4(a) will gradually increase and then decrease as the increase of the distance and the influence of dark counts will be more obvious after 250 m. Because the attenuation of background light is a bit smaller than that of the signal. The QBERs for the optimal system are illustrated in Fig.4 (d), (e),(f). When the

distance is about 300 m, which is within the maximum estimated distance for underwater quantum communication[15, 26], the main sources of the QBER will be the background light and dark counts for underwater QKD. Low dark counts and background light, limited by gate time and filter spectral width, for the optimal system make it possible for long distance (i.e 300m) QKD in the clearest ocean water. For underwater environment, reducing the dark counts and background light can reduce the QBER effectively, which is effective for remote QKD.

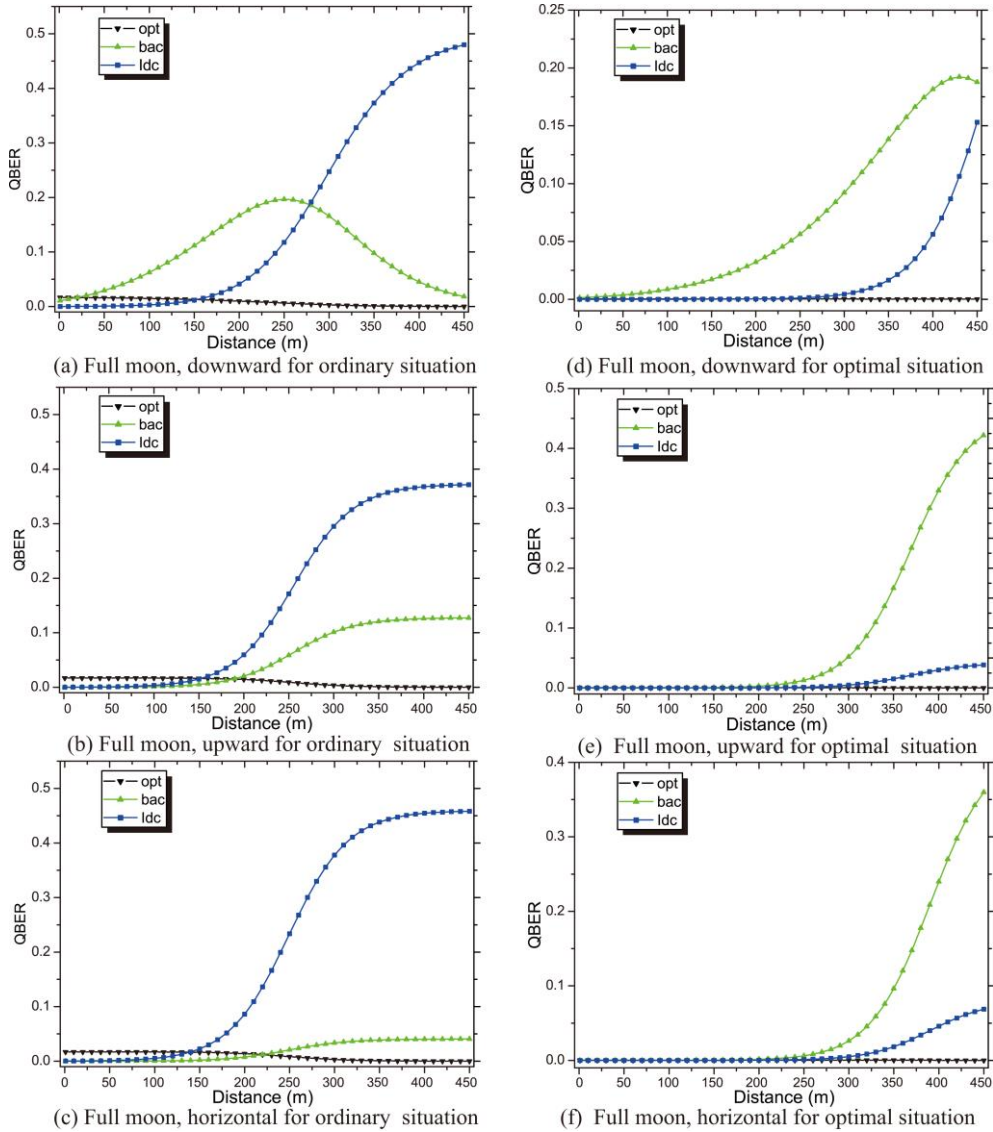


Fig. 4. (color online)QBER come from different factors,  $Q_{opt}$ ,  $Q_{bac}$ ,  $Q_{ldc}$  as a function of propagation distance under full moon condition with an attenuation coefficient of 0.03/m. (a), (b), (c) are calculated according the parameters shown in Table 1 and (d), (e), (f) are calculated according the parameters shown in Table 2

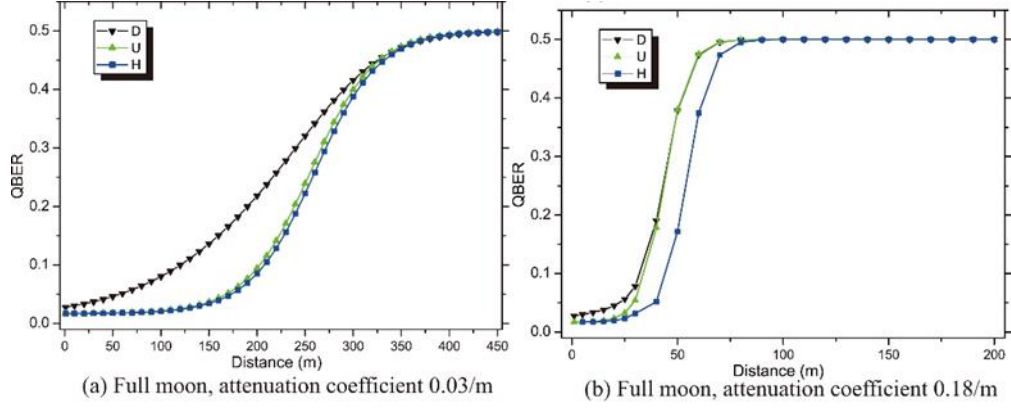


Fig. 5. The total QBER of underwater QKD in Jerlov type seawater for the ordinary case with the different attenuation coefficient. (a).  $\chi_c = 0.03/m$ . (b).  $\chi_c = 0.18/m$ . The parameters we used to do the calculation are shown in Table 1.

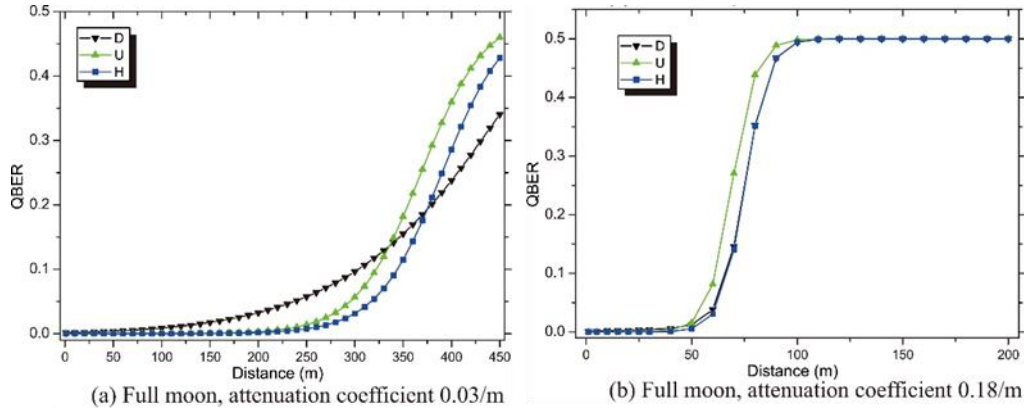


Fig. 6. (color online)The total QBER of underwater QKD in Jerlov type seawater for the optimal case with the different attenuation coefficient. (a).  $\chi_c = 0.03/m$ . (b).  $\chi_c = 0.18/m$ . The parameters we used to do the calculation are shown in Table 2.

In order to determine the distance of secure QKD, we further calculate the total QBER under different conditions. The results are shown in Fig. 5 and 6. The QBER of the optimal system is smaller than that of the ordinary system because both of the dark counts and detected background light are smaller than that of the ordinary system. For the ordinary system the QBER will reach 11% when the distance is about 130 m for the downward mode and about 200 m for other two modes when the attenuation coefficient is 0.03/m. The distance can reach as long as more than 300m if we improved the performance of the system. See Fig. 5(a) and Fig.6 (a) for more details. While for the seawater with an attenuation coefficient of 0.18/m, the secure QKD distance is only a few tens of meters in both cases because of severe attenuation . It is obvious that the QBER of the downward mode is the highest among the three modes, because the background light is strongest when the secure

underwater QKD performed.

## B. Analysis of the key rate of underwater QKD

In BB84 protocol, the sifted key rate is [18, 27]

$$k = f \cdot \mu \cdot T_{link} \cdot q \cdot (1 - QBER) \cdot \frac{\eta}{2} \cdot \eta_{opt}, \quad (7)$$

where  $f$  is the pulse frequency of the laser,  $T_{link}$  is the transmission ratio of seawater channel,  $q$  is the sifting factor which is usually  $\leq 1$  and typically 1 or 1.2, and  $k$  is the rate of sifted key. In this paper, the value of  $q$  is taken as 1. With the QBER shown in Fig.5 and 6, we can obtain the sifted key rate of underwater QKD, which is illustrated in Fig. 7.

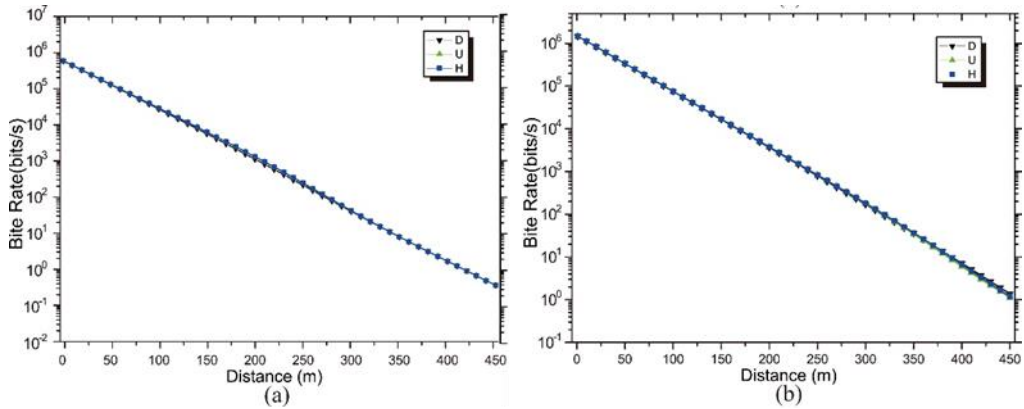


Fig. 7. The sifted key rates as a function of propagation distance in clear Jerlov type-I seawater, under full moon condition. The lines with up triangles, down triangles and squares represent upward, downward and horizontal communication modes, respectively. (a) is calculated according the parameters shown in Table 1 and (b) is calculated according the parameters shown in Table 2.

The sifted key rate of underwater QKD in the ordinary case is about 27 kbit/s at a distance of 100m, which can reach around 76 kbit/s in the optimal case. The results will be a bit different for different lunar phase angles. As shown in Fig 7, the sifted key rate for the three modes are almost the same because the difference of the three modes is the QBER, whose influence on the sifted key rate is linearity, which is far smaller than that of the attenuation of the water channel which obeys Beer-Lambert law [21, 28].

Then, the final key rate for practical QKD with decoy state can be estimated according to the GLLP formula [29, 30]:

$$R \geq q[-Q_\mu f(E_\mu) H_2(E_\mu) + Q_1[1 - H_2(e_1)]], \quad (8)$$

where  $Q_\mu$  is the gain of signal states,  $E_\mu$  is the QBER of singal states,  $Q_l$  is the gain of single-photon states,  $e_1$  is the error rate of single photons,  $f(E_\mu)$  is the error correction efficiency and  $f(E_\mu) \geq 1$ ,  $H_2(x) = -x \log_2(x) - (1-x) \log_2(1-x)$ . is the binary Shannon entropy. For the QKD without decoy states, the final key will be [29, 30]:

$$R \geq Q_\mu \cdot [-f(E_\mu)H_2(E_\mu) + \Omega(1 - H_2(E_\mu / \Omega))], \quad (9)$$

where  $\Omega$  is the fraction of “untagged” photons. Then the final key rate in clearest Jerlov type I seawater can be calculated, which is shown in Fig. 8.

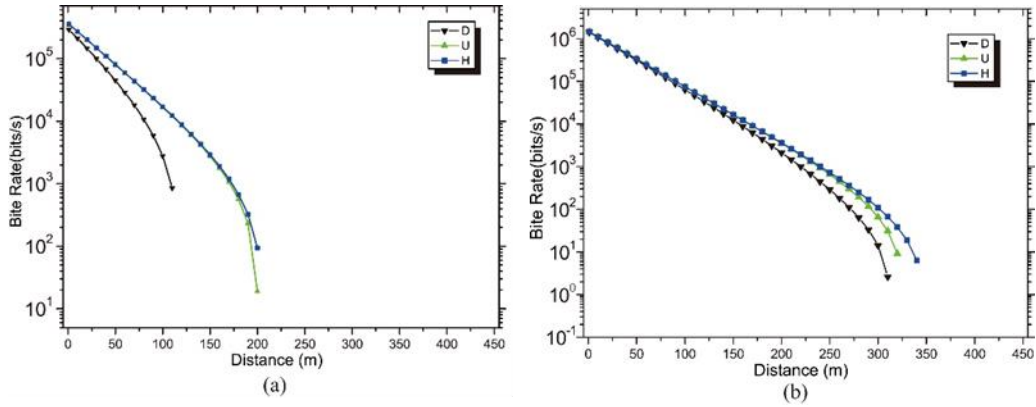


Fig. 8. Final key rate of underwater QKD in the ordinary case (a) and in the optimal case (b). (a) is calculated according the parameters shown in Table 1 and (b) is calculated according the parameters shown in Table 2

For the ordinary system, the security key rate is about 2.7 kbit/s when the propagation distance is 100 m for the downward mode and approximate 16 kbit/s for the other two modes. For the optimal optical parameters, the key rate can reach 56.7 kbit/s for downward mode and about 67 kbit/s for upward and horizontal modes at a distance of 100 m. The maximum secure distance can reach about 310 m, 320 m and 340 m for downward, upward and horizontal modes, respectively. For practical QKD with decoy state, the final key rate, which can be estimated according to Eq. 8, will be improved. Considering the simple onedecoy

protocol [30], we have  $Q_l = \mu e^{-\mu} Y_l$ ,  $E_l = \frac{E_\nu Q_\nu e^\nu}{Y_l \nu}$ , where  $Y_l = \frac{\mu}{\mu \nu - \nu^2} (Q_\nu e^\nu - Q_\mu e^\mu \frac{\nu^2}{\mu^2})$ ,  $\mu$

and  $\nu$  represent the mean photon number per pulse of signal state and decoy state, respectively. (a) Full moon, attenuation coefficient 0.03/m (b) Full moon, attenuation coefficient 0.18/m Fig. 6. (color online) The total QBER of underwater QKD in Jerlov type seawater for the optimal case with the different attenuation coefficient. (a).  $\chi_c = 0.03/m$ . (b).  $\chi_c = 0.18/m$ . The parameters we used to do the calculation are shown in Table 2. We calculate

the final key for the ordinary case according to Table.1 under full moon condition when  $\mu = 0.48$  and  $\nu = 0.05$ . The results show that the final key rate can reach 13.7kbits/s, 31.7kbits/s and 31.5kbits/s at the distance of 100m for upward, downward and horizontal modes, respectively.

## 6. CONCLUSION AND DISCUSSION

In this paper, we firstly modify the formula to calculate the QBER. Then we analyse the influence of imperfect optical elements on polarization states and study the background light underwater in detail using Hydrolight. At last, we investigate the performance of underwater QKD according to the modified formula. Though the final key rate is very low in our case, it can be increased by increasing the pulse repetition rate  $f$ . The performance of underwater QKD will be improved if decoy states are applied, and it is also important to improve the performance of the polarization elements and single photon detector. With the increasing of the final key rate and secure communication distance, it is possible to take the underwater quantum communication into practice in the future. Attenuation coefficient is affected by wavelength and the light we analyzed is 480nm in this paper, which is in the blue-green optical window of seawater. If another wavelength is selected, the results will be different and can also be calculated accordingly. Besides, the type of seawater will also affect the attenuation coefficient because the main component will differ for different types of seawater and the absorption peak will change for different component. The results show improving the performance of the optical elements, especially the performance of the detector, will be helpful to implement underwater QKD. Besides, the synchronous signal is also necessary for underwater QKD. To avoid the influence of the synchronous signal on the QBER, another wavelength, also in blue-green range, is necessary and the time delay between quantum signal and synchronous signal is also essential. For practical underwater environment, there will be (a) (b) Fig. 8. Final key rate of underwater QKD in the ordinary case (a) and in the optimal case (b). (a) is calculated according the parameters shown in Table 1 and (b) is calculated according the parameters shown in Table 2. many other factors affecting the propagation of beam light for underwater QKD, such as dot whipping caused by turbulence, distortion of wavefront, etc. These factors may cause depolarization and extra loss, then the QBER and key rate will be affected accordingly. Therefore, auxiliary optical system is necessary to minimize the influence, such as the APT(acquiring, pointing and tracking) system, which is widely used in free space communications.

## ACKNOWLEDGMENTS

This work was supported by the National Natural Science Foundation of China (Grant Nos. 61575180, 61701464 and 11475160 ).

## REFERENCES

1. C. H. Bennett, and G. Brassard, "Quantum cryptography: Public key distribution and coin tossing," Proceedings of the IEEE International Conference on Computers, Systems and Signal Processing, IEEE, New York, 560 175-179 (1984).
2. H.K.Lo and H.F. Chau, "Unconditional security of quantum key distribution over arbitrarily long distances," *Science*, 283, 2050-2056(1999).
3. P. W. Shor and J. Preskill, "Simple proof of security of the BB84 quantum key distribution protocol," *Physical Review Letters*, 85, 441- 444(2000).
4. D.Gottesman, H. K. Lo, N. Lutkenhaus, and J. Preskill, "Security of quantum key distribution with imperfect devices," *Quantum Information and Computation*, 4, 325-360(2004).
5. C. H. Bennett, and G. Brassard, "Experimental quantum cryptography: the dawn of a new era for quantum cryptography: the experimental prototype is working," *Sigact News* 37, 78-80 (1989).
6. H. Takesue, E.Diamanti, C. Langrock, M. M. Fejer and Y. Yamamoto, "10-GHz clock differential phase shift quantum key distribution experiment," *Optics Express*, 14, 9522-9530(2006).
7. H. Takesue, S. W. Nam, Q. Zhang, R. H. Hadfield, T. Honjo, K. Tamaki, &Y. Yamamoto, "Quantum key distribution over a 40-dB channel loss using superconducting single-photon detectors," *Nature Photonics*, 1, 343-348(2007).
8. S. Wang, W. Chen, J. F. Guo, Z. Q. Yin, H. W. Li, Z. Zhou, G. C. Guo, and Z. F. Han, "2 GHz clock quantum key distribution over 260 km of standard telecom fiber," *Opt. Lett.* 37, 1008 (2012).
9. E. Gibney, "Chinese Satellite Is One Giant Step for the Quantum Internet," *Nature*, 535(7613):478(2016).
10. S. K. Liao, W. Q. Cai, W. Y. Liu, L. Zhang, Y. Li, J. G. Ren, J. Yin, Q. Shen, Y. Cao, Z. P. Li, F. Z. Li, X. W. Chen, L. H. Sun, J. J. Jia, J. C. Wu, X. J. Jiang, J. F. Wang, Y. M. Huang, Q. Wang, Y. L. Zhou, L. Deng, T. Xi, L. Ma, T. Hu, Q. Zhang, Y. A. Chen, N. L. Liu, X. B. Wang, Z. C. Zhu, C. Y. Lu, R. Shu, C. Z. Peng, J. Y. Wang and J. W. Pan, "Satellite-to-

ground quantum key distribution," *Nature* 549.7670(2017).

11. J. Yin, Y. Cao, Y. H. Li, S. K. Liao, L. Zhang, J. G. Ren, W. Q. Cai, W. Y. Liu, B. Li, H. Dai, G. B. Li, Q. M. Lu, Y. H. Gong, Y. Xu, S. L. Li, F. Z. Li, Y. Y. Yin, Z. Q. Jiang, M. Li, J. J. Jia, G. Ren, D. He, Y. L. Zhou, X. X. Zhang, N. Wang, X. Chang, Z. C. Zhu, N. L. Liu, Y. A. Chen, C. Y. Lu, R. Shu, C. Z. Peng, J. Y. Wang and J. W. Pan, "Satellitebased entanglement distribution over 1200 kilometers," *Science*, 356. 6343(2017).
12. M. Lanzagorta, "Underwater Communications," Morgan & Claypoo (2012).
13. U. Jeffrey, M. Lanzagorta, and S. E. Venegas-Andraca. "Quantum communications in the maritime environment." *OCEANS'15 MTS/IEEE Washington*. IEEE, (2015).
14. S. Peng, S. C. Zhao, Y. J. G and W. D. Li, "Channel analysis for single photon underwater free space quantum key distribution," *JOSA A*, 32(3):349-56(2015).
15. L. Ji, J. Gao, A. L. Yang, Z. Feng, X. F. Lin, Z. G. Li and X. M. Jin, "Towards quantum communications in free-space seawater," *Opt. Express* 25, 19795-19806 (2017)
16. C. D. Mobley, "Light and Water: Radiative Transfer in Natural Waters," Academic Press(1994).
17. D. J. Rogers, J. C. Bienfang, A. Mink, B. J. Hershman, A. Nakassis, X. Tang, L. Ma, D. H. Su, C. J. Williams and C. W. Clark, "FreeSpaceQuantum Cryptography in the H-alpha FraunhoferWindow," *Proceedings of SPIE*, 6304, 630417(2006).
18. N. Gisin, G. Ribordy, W. Tittel, and H. Zbinden, "Quantum Cryptography," *Rev. Mod. Phys.* 74, 175(2001).
19. S. D. Miller and R. E. Turner, "A Dynamic Lunar Spectral Irradiance Data Set for NPOESS/VIIRS Day/Night Band Nighttime Environmental Applications," *IEEE Transactions on Geoscience & Remote Sensing*, 47(7):2316-2329(2009).
20. P. F. Liao, and G. Hermann, "Polarized Light," &The Optics Encyclopedia(2005).
21. W. G. Driscoll, W. Vaughan and M. E. Cox, "Handbook of Optics," American Journal of Physics(1979).
22. <https://www.newport.com.cn/f/quartz-zero-order-quarter-wave-plates>.
23. [https://www.thorlabschina.cn/newgroupage9.cfm?objectgroup\\_id=7234](https://www.thorlabschina.cn/newgroupage9.cfm?objectgroup_id=7234).
24. J. H. Shi, Z. P. Wang, and C. Y. Guan, "Theoretical analysis of nonpolarizing beam splitters with appropriate amplitude and phase," *Optics & Laser Technology*, 41(3):351-355(2009).

25. O.Kahl, S. Ferrari, V. Kovalyuk, G. N. Goltsman, A. Korneev and W. H. Pernice, "Waveguide integrated superconducting single-photon detectors with high internal quantum efficiency at telecom wavelengths. " *Scientific Reports* 5:10941(2015).
26. H. K. Lo, M. Curty, and K. Tamaki, "Secure quantum key distribution," *Nature Photon.* 8, 595–604 (2014).
27. V. Scarani, H. Bechmann-Pasquinucci, N. J. Cerf, M. Dusek, N. Lütkenhaus and M. Peev, "The security of practical quantum key distribution," *Reviews of modern physics*, 81(3): 1301(2009).
28. M. Bass, E. W. Van Stryland and D. R. Williams, "Handbook of optics," New York: McGraw-Hill, (1995).
29. H. K. Lo, X. Ma and K. Chen, "Decoy state quantum key distribution". *Physical review letters*, 94(23): 230504(2005).
30. X.Ma, B. Qi, Y. Zhao and H. K. Lo, "Practical decoy state for quantum key distribution". *Physical Review A*, 72(1), 012326(2005).